

Experimental and Clinical Radiofrequency Ablation: Proposal for Standardized Description of Coagulation Size and Geometry

Stefaan Mulier, MD,¹ Yicheng Ni, MD, PhD,¹ Lars Frich, MD,² Fernando Burdio, MD,³
Alban L. Denys, MD,⁴ Jean-François De Wispelaere, MD,⁵ Benoît Dupas, MD, PhD,⁶
Nagy Habib, MD, FRCS,⁷ Michael Hoey, PhD,⁸ Maarten C. Jansen, MD,⁹
Marc Lacrosse, MD,⁵ Raymond Leveille, MD,¹⁰ Yi Miao, MD, PhD,¹¹
Peter Mulier,¹² Didier Mutter, MD, PhD,¹³ Kelvin K. Ng, MBBS, PhD, FRCSEd (Gen),¹⁴
Roberto Santambrogio, MD,¹⁵ Dirk Stippel, MD,¹⁶ Katsuyoshi Tamaki, MD,¹⁷
Thomas M. van Gulik, MD,⁹ Guy Marchal, MD, PhD,¹ and Luc Michel, MD, FACS¹⁸

¹Department of Radiology, Gasthuisberg University Hospital, Herestraat 49, 3000 Leuven, Belgium

²Department of Surgery, Rikshospitalet University Hospital, Sognsvannsveien 20, 0027 Oslo, Norway

³Unity of Liver Surgery and Liver Transplantation, Bellvitge University Hospital, Feixa Llarga, sn, 08907 Hospitalet de Llobregat, Barcelona, Spain

⁴Department of Diagnostic and Interventional Radiology, Centre Hospitalier Universitaire Vaudois, Rue du Bugnon 46, 1011 Lausanne, Switzerland

⁵Department of Radiology, Mont-Godinne University Hospital, Avenue du Dr. Thérasse 1, 5530 Yvoir, Belgium

⁶Central Service of Radiology and Medical Imaging, Hôtel Dieu, University Hospital of Nantes, Place Alexis Ricordeau 1, 44093 Nantes Cedex 01, France

⁷Department of Liver and Pancreas Surgery, Imperial College London, Hammersmith Hospital, Du Cane Road, W12 0NN London, UK

⁸Biomedical Engineer, 5733 Pond Drive, Shoreview, Minnesota 55126, USA

⁹Department of Surgery, Academic Medical Center, Meibergdreef 9, 1105 AZ Amsterdam, The Netherlands

¹⁰Division of Endourology, Laparoscopy and Minimally Invasive Surgery, University of Miami School of Medicine, Professional Arts Center, 1150 NW 14th Street, Suite 309, Miami, Florida 33101, USA

¹¹Department of General Surgery, The First Affiliated Hospital of Nanjing Medical University, Nanjing 210029, China

¹²Biomedical Engineer, 8140 Lake Elmo Avenue, Stillwater, Minnesota 55082, USA

¹³Department of General Surgery, University Hospital of Strasbourg, Place de l'Hôpital, 67091 Strasbourg Cedex, France

¹⁴Department of Surgery, University of Hong Kong, Queen Mary Hospital, 102 Pofulam Road, Hong Kong 852, China

¹⁵Unit of Bilio-pancreatic Surgery, Ospedale San Paolo, University of Milan, via A. di Rudini 8, 20142 Milan, Italy

¹⁶Department of Visceral and Vascular Surgery, University of Cologne, Joseph Stelzmann Strasse 9, 50924 Cologne, Germany

¹⁷Department of Digestive and Cardiovascular Medicine, Tokushima University School of Medicine, (3-18-15) Kuramoto-cho, Tokushima 770-8503, Japan

¹⁸Department of Surgery, Mont-Godinne University Hospital, Avenue du Dr. Thérasse 1, 5530 Yvoir, Belgium

Background: Radiofrequency (RF) ablation is used to obtain local control of unresectable tumors in liver, kidney, prostate, and other organs. Accurate data on expected size and geometry of coagulation zones are essential for physicians to prevent collateral damage and local tumor recurrence. The aim of this study was to develop a standardized terminology to describe the size and geometry of these zones for experimental and clinical RF.

Received October 19, 2005; accepted April 3, 2006

Address correspondence and reprint requests to: Luc Michel, MD, FACS; E-mail: michel@chir.ucl.ac.be

Published by Springer Science+Business Media, Inc. © 2007 The Society of Surgical Oncology, Inc.

Methods: In a first step, the essential geometric parameters to accurately describe the coagulation zones and the spatial relationship between the coagulation zones and the electrodes were defined. In a second step, standard terms were assigned to each parameter.

Results: The proposed terms for single-electrode RF ablation include *axial diameter, front margin, coagulation center, maximal and minimal radius, maximal and minimal transverse diameter, ellipticity index, and regularity index*. In addition a subjective description of the general shape and regularity is recommended.

Conclusions: Adoption of the proposed standardized description method may help to fill in the many gaps in our current knowledge of the size and geometry of RF coagulation zones.

Key Words: Radiofrequency ablation—Tumor ablation—Size—Geometry—Liver—Kidney.

Radiofrequency ablation (RF ablation) is a valuable technique to obtain local control of unresectable tumors in liver,^{1–7} kidney,⁸ prostate,⁹ and other organs. An important clinical limitation is the inability to monitor the growing coagulation zone accurately during the procedure. Real-time monitoring of the area of coagulation with ultrasound is unreliable.^{10–13} A too small coagulation zone will inevitably lead to local recurrence.² Although local recurrence is lower than 10% in the best series,^{1,2,4–7} in other series it can be as high as 60%.^{14,15} On the other hand, a too large coagulation zone may lead to collateral damage.^{3,16–18} Therefore, exact knowledge of the expected size and geometry of coagulation zones is essential to correctly prepare and perform the intervention. A recent review showed that much of this crucial information is lacking for the current commercial RF ablation electrodes.¹⁹ The aim of this study was to develop and propose an optimal set of descriptive parameters for different RF ablation electrodes and protocols. The second aim was to standardize description terminology.

MATERIALS AND METHODS

For *experimental RF ablation*, the optimal set of descriptive parameters for coagulation zones created by single and dual electrodes²⁰ was developed. This set was defined as the minimal information needed to accurately document the coagulation zone size and geometry. We adopted the principle that not only the coagulation zone but also the *spatial relationship* of the coagulation zone *with the electrode(s)* should be described.

In a second step, a standard term was assigned to each parameter. This term had to match predefined quality criteria and was either chosen from the literature, if available, or newly created. Therefore, we carried out a PubMed search for the period from

January 1, 1990, to May 1, 2005, using the key words radiofrequency (or radio-frequency or radio frequency) and liver (or hepatic or hepatocellular) on articles written in English, French, German, Italian, Spanish, Danish, or Dutch. Relevant papers were also identified from the reference lists of the papers previously obtained through the search. Only papers with a main aim to describe the *in vivo* and *ex vivo* coagulation zones after a single RF ablation session in animal liver with commercial or experimental electrodes were retained. Publications using both single electrodes and multiple-electrode systems²⁰ were included. For each parameter, numerous synonyms were found in the literature. In order to distill the most unequivocal term for each parameter, we first rejected synonyms that suggested a ranking of size, such as “long(est) axis” and “short(est) axis”, because the longest axis does not necessarily correspond to the axial diameter; neither does the shortest axis always correspond to the transverse diameter.^{19,21} We then rejected synonyms that suggested a position in space, such as “vertical diameter”, because an RF ablation electrode can be inserted in any direction in the laboratory as well as in a patient. Thirdly, from the remaining terms, the most “expressive” and “intuitively suggestive” term was selected. Finally, some lacking terms had to be newly created.

For *clinical RF ablation*, applicability of these experiment-derived definitions to the clinical setting was studied.

RESULTS

Current Unstandardized Descriptive Parameters in the RF Ablation Literature

Up to 12 synonyms were identified for describing the same parameter of the coagulation zone. For other valuable parameters, no terms at all were available (Tables 1–5).

TABLE 1. Description of experimental coagulation zones made by a single electrode

Current proposal	Abbreviation	Synonyms	References
Measurements in axial plane			
Axial diameter	AD	Length, longitudinal dimension/diameter, long axis diameter, longest axis length, maximum diameter, short axis diameter, shortest axis length, depth, height, vertical diameter, vertical axis diameter	11, 12, 19, 21–47, Curley unpublished data
Front margin	FM	Relation to electrode tip, distance of ablation beyond electrode tip	19, 22
Coagulation center	CC		
Measurements in transverse plane			
Minimal transverse diameter	TD _{min}	Width, diameter, short axis diameter, shortest diameter, shortest axis length, minimum diameter, long axis diameter, longest axis length, depth, height, perpendicular diameter, anterior-posterior diameter	11, 12, 19, 21–25, 27–33, 35–38, 40, 42–44, 46, 48–52
Maximal transverse diameter	TD _{max}	Idem as above	11, 12, 19, 21–25, 27–33, 35–38, 40, 42–44, 46, 48–55
Minimal radius	R _{min}		19
Maximal radius	R _{max}		19
General shape in axial plane			
Ellipticity index	EI	Aspect ratio, shape value	19, 56, 57
Regularity of shape in transverse plane			
Regularity index	RI		

TABLE 2. Description of experimental coagulation zones made by a dual-electrode system

Current proposal	Abbreviation	Synonyms	References
Measurements in axial plane			
Axial diameter	AD1, AD2	Longest diameter along electrode, short axis diameter, vertical diameter	58–62
Front margin	FM1, FM2		
Mid-axial diameter	MAD	Shortest diameter at midpoint, shortest diameter midway between the two electrodes, height	58, 60, 63, 64
Measurements in transverse plane			
Inline transverse diameter	ITD	Long(est) axis diameter, length, overlapping width	58–63, 65
Lateral margin	LM1, LM2		
Perpendicular transverse diameter	PTD1, PTD2	Short axis diameter, width	59, 61–63, 65
Mid-transverse diameter	MTD		
General shape in axial plane			
Axial fusion index	AFI		
General shape in transverse plane			
Transverse fusion index	TFI		

Proposal for Standardized Description

Experimental RF Ablation: Minimal Descriptive Parameters

In order to obtain accurate measurements that can be related to the position of the electrode, the electrode should be left in place until the liver is sectioned (Table 1). The tines of expandable electrodes are withdrawn into the shaft. With the knife shaving the electrode, the liver is first cut along an *axial plane*, which is defined as a plane along the electrode axis (Fig. 1). Measurements are performed and pictures are taken. All measurements include the central tan-white zone, which corresponds to irreversibly dam-

aged tissue, and exclude the surrounding hyperaemic red rim (for in vivo experiments), which corresponds to viable tissue on acute histochemical staining.²² Coagulation zones that extend to the liver surface should not be taken into account for measurement since the obtained measurements represent an underestimation of the size the coagulation zone would reach in the middle of the parenchyma. Measurements can be performed macroscopically using calipers or on digital photographs using public domain software packages such as ImageJ (National Institutes of Health, Bethesda, MD; <http://www.rsb.info.nih.gov/ij/> [accessed May 16, 2006]) or commercially available image analysis software.

TABLE 3. Description of clinical coagulation zones made by a single electrode

Current proposal	Abbreviation	Synonyms	References
Measurements in axial plane of the electrode			
Axial diameter	AD ^{el}	Length, longitudinal dimension/diameter, long axis diameter, longest axis length, maximum diameter, short axis diameter, shortest axis length, depth, height, vertical diameter, vertical axis diameter	11, 12, 19, 21–47, Curley unpublished data
Measurements in transverse plane of the electrode			
Minimal transverse diameter	TD _{min} ^{el}	Width, diameter, short axis diameter, shortest diameter, shortest axis length, minimum diameter, long axis diameter, longest axis length, depth, height, perpendicular diameter, anterior-posterior diameter	11, 12, 19, 21–25, 27–33, 35–38, 40, 42–44, 46, 48–52
Maximal transverse diameter	TD _{max} ^{el}	Idem as above	11, 12, 19, 21–25, 27–33, 35–38, 40, 42–44, 46, 48–55
General shape in axial plane of the electrode			
Ellipticity index	EI ^{el}	Aspect ratio, shape value	19, 56, 57

In clinical reports, “axial” and “transverse” describe the spatial relation with the axis of the electrode and not the spatial relation with the axis of the patient. The exposant “el” is added to the abbreviations for clarity.

TABLE 4. Frequency of use of proposed descriptive parameters in experimental RF ablation literature, single electrode

Parameter	Percentage	No. studies
All studies	100%	50
Measurements in axial plane		
Axial diameter	36%	18
Front margin	2%	1
Coagulation center	0%	0
Measurements in transverse plane		
Minimal transverse diameter	10%	5
Maximal transverse diameter	24%	12
Minimal radius	0%	0
Maximal radius	0%	0
General shape in axial plane		
Ellipticity index	10%	5
Regularity of shape in transverse plane		
Regularity index	0%	0

TABLE 5. Frequency of use of proposed descriptive parameters in experimental RF ablation literature, dual-electrode system

Parameter	Percentage	No. studies
All studies	100%	10
Measurements in axial plane		
Axial diameter	60%	6
Front margin	0%	0
Mid-axial diameter	40%	4
Measurements in transverse plane		
Inline transverse diameter	70%	7
Lateral margin	0%	0
Perpendicular transverse diameter	0%	0
Mid-transverse diameter	60%	6
General shape in axial plane		
Axial fusion index	0%	0
General shape in transverse plane		
Transverse fusion index	0%	0

Measurements should be performed before histological tissue fixation with associated tissue shrinkage.

Second, both halves of the coagulation zone are cut in the *transverse plane*, which is defined as the plane perpendicular to the electrode (and to the axial plane) at the site of the largest transverse diameter of the coagulation zone. The two quarters nearest to the electrode tip are then reassembled; measurements are performed and pictures are taken.

Measurements in the Axial Plane (Fig. 2A)

The *axial diameter (AD)* is defined as the distance in mm between the proximal and the distal edges of the coagulation zone, in the axis of the electrode.

The *front margin (FM)* is defined as the distance in mm between the distal edge of the coagulation zone and the electrode tip. For expandable electrodes, the tines are not taken into account.

The *coagulation center (CC)* is defined as the section point of the transverse plane and the electrode (axis). Its position is expressed as the distance in mm of the CC to the electrode tip. In other words, its position is measured as the distance between the projection of the site of the maximal transverse diameter on the electrode (axis) and the electrode tip. For expandable electrodes, the tines are not taken into account. The value is positive when the CC is distal to the electrode tip, i.e., into the tissue, and

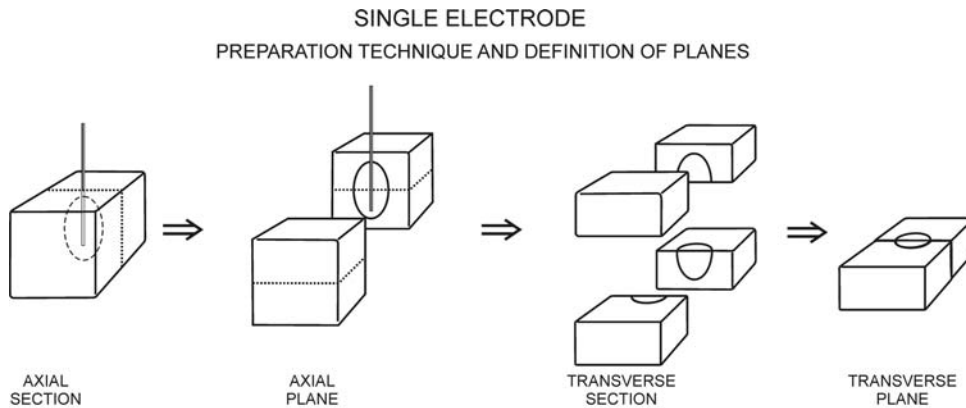


FIG. 1. Preparation technique and definition of planes for single-electrode RF ablation.

negative when it is proximal to the electrode tip, i.e., on the electrode itself.

Measurements in the Transverse Plane (Fig. 2B)

The *maximal radius* (R_{max}) is defined as the maximal distance in mm between the electrode shaft and the edge of the coagulation zone in the transverse plane.

The *minimal radius* (R_{min}) is defined as the minimal distance in mm between the electrode shaft and the edge of the coagulation zone in the transverse plane. Maximal and minimal radii are not necessarily perpendicular to each other.

The *maximal transverse diameter* (TD_{max}) is defined as the maximal distance in mm between two opposite edges of the coagulation zone in the transverse plane.

The *minimal transverse diameter* (TD_{min}) is defined as the minimal distance in mm between two opposite edges of the coagulation zone in the transverse plane, measured on a line crossing halfway the line of the maximal transverse diameter.

Both transverse diameters cross at the center of the coagulation zone. This center does not necessarily correspond to the site of the electrode shaft. The maximal and minimal transverse diameters are not necessarily perpendicular to each other.

General Shape in the Axial Plane (Fig. 2C)

The *ellipticity index* (EI) quantitatively describes the general coagulation zone shape in the axial plane and is calculated as the ratio of axial diameter (AD) and mean transverse diameter $[(TD_{min} + TD_{max})/2]$:

$$EI = 2AD / (TD_{min} + TD_{max})$$

Provided that TD_{min} is close to TD_{max} , a ratio of 1.0 roughly corresponds to a spherical coagulation zone; a ratio > 1.0 , to an elliptical coagulation zone; and a ratio < 1.0 , to a flattened sphere.

Regularity of Shape in the Transverse Plane (Fig. 2D)

The *regularity index* (RI) quantitatively describes the regularity of the coagulation zone shape in the transverse plane and is calculated as the ratio of R_{min} and R_{max} :

$$RI = R_{min} / R_{max}$$

This way, a ratio close to 1.0 corresponds to a nearly spherical coagulation zone. The lower the ratio, the more irregular the coagulation zone (asymmetrical, with indentations, or with extensions). For a ratio inferior to 0.80, the (most frequently found) type(s) of irregularity should be specified in the subjective description (see further).

Dual-Electrode System (Table 2)

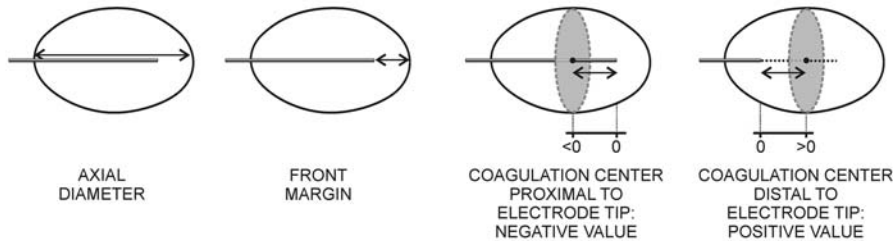
A dual-electrode system is defined as the combined use of two single electrodes inserted into the target tissue, either monopolar or bipolar.²⁰ Only electrodes inserted in parallel are considered here.

Preparation Technique and Definition of Planes (Fig. 3)

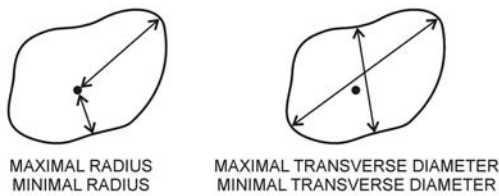
The preparation technique is similar as described above for single electrodes, except for the following steps. The coagulation zone is first cut along the *axial plane*, which is defined as the plane along both electrode axes. Measurements are performed and pictures are taken. Then, both halves of the coagulation zone are cut in the *transverse plane*, which is defined as the plane perpendicular to the electrode axes at the site of the largest transverse diameter of the coagulation zone in the axial plane. The two quarters nearest to the electrode tip are then reassembled; measurements are performed and pictures are taken.

SINGLE ELECTRODE
DESCRIPTION OF COAGULATION ZONE

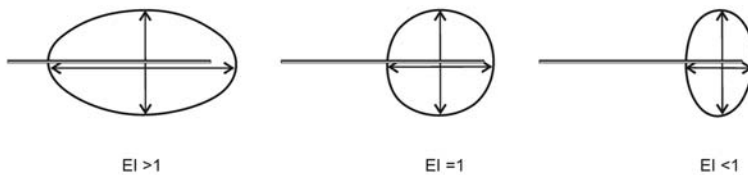
A) DIMENSIONS IN AXIAL PLANE



B) DIMENSIONS IN TRANSVERSE PLANE



C) ELLIPTICITY INDEX



D) REGULARITY INDEX

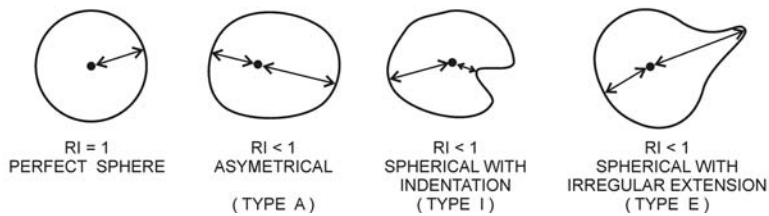


FIG. 2. Description of coagulation zones made by a single electrode.

Measurements in the Axial Plane (Fig. 4A)

The *axial diameter* ($AD1$, $AD2$) is defined as the distance in mm between the proximal and the distal edges of the coagulation zone, and in the axis of one electrode. It is measured for both electrodes.

The *front margin* ($FM1$ and $FM2$) is defined as the distance in mm between the distal edge of the coagulation zone and the electrode tips. For expandable electrodes, the tines are not taken into account. It is measured for both electrodes.

The *mid-axial diameter* (MAD) is defined as the distance in mm between the proximal and the distal edges of the coagulation zone, in the axis halfway and parallel to both electrodes.

Measurements in the Transverse Plane (Fig. 4B)

The *inline transverse diameter* (ITD) is defined as the distance in mm between the edges of the coagulation zone in the interelectrode axis in the transverse plane.

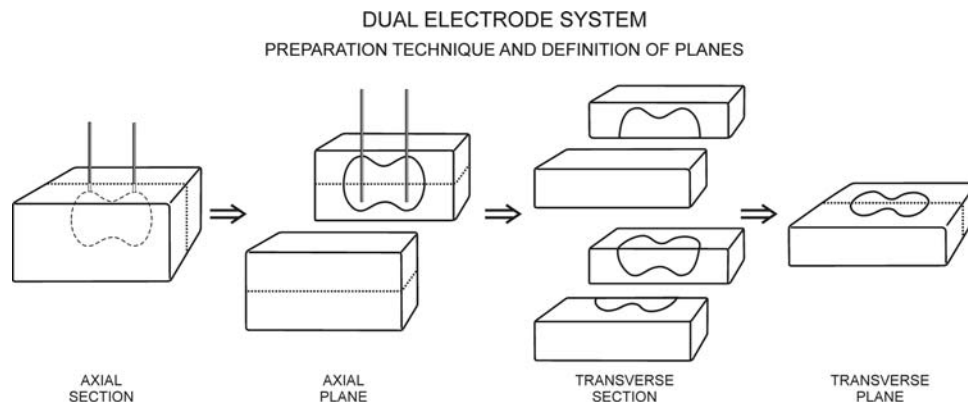


FIG. 3. Preparation technique and definition of planes for dual-electrode RF ablation.

The *lateral margin* ($LM1$ and $LM2$) is defined as the distance in mm between the edges of the coagulation zone and the electrode in the interelectrode axis in the transverse plane. It is measured for both electrodes.

The *perpendicular transverse diameter* ($PTD1$ and $PTD2$) is defined as the diameter of the coagulation zone perpendicular to the interelectrode axis where it crosses an electrode in the transverse plane. It is measured for both electrodes.

The *mid-transverse diameter* (MTD) is defined as the diameter of the coagulation zone perpendicular to the interelectrode axis halfway between both electrodes in the transverse plane.

General Shape in the Axial Plane (Fig. 4C)

The *axial fusion index* (AFI) quantitatively describes the completeness of fusion of the coagulation zones around each electrode in the axial plane and is calculated as the ratio of the mid-axial diameter (MAD) and the mean AD $[(AD1 + AD2)/2]$:

$$AFI = 2MAD/(AD1 + AD2)$$

This way, a ratio ≥ 1.0 corresponds to complete fusion and a ratio < 1.0 to incomplete fusion.

General Shape in the Transverse Plane (Fig. 4D)

The *transverse fusion index* (TFI) quantitatively describes the completeness of fusion of the coagulation zones around each electrode in the transverse plane and is calculated as the ratio of the mid-transverse diameter (MTD) and the mean: PTD $[(PTD1 + PTD2)/2]$

$$TFI = 2MTD / (PTD1 + PTD2)$$

This way, a ratio ≥ 1.0 corresponds to complete fusion and a ratio < 1.0 , to incomplete fusion.

Multiple (> 2) Electrode System

A multiple (> 2) electrode system is defined as the combined use of more than two single electrodes inserted into the target tissue.²⁰ As these systems can be used in a very versatile way, the description should be individualized to each system, bearing in mind the goal to offer to the clinician accurate and clinically useful descriptive parameters, which should always be related to the position of the electrodes. For example, a coagulation zone created by three symmetrically inserted electrodes close to each other can be described as if it was created by a single electrode. A coagulation zone created by three symmetrically inserted electrodes further from each other can be described using elements of the proposed description for a dual-electrode system. However, a coagulation zone created by four or more electrodes, or asymmetrically placed electrodes, requires an individualized description.

Variability

Each parameter should be presented as *mean value \pm standard deviation (SD)*. In papers that compare different electrodes or protocols, the *Coefficient of Variation (CV)* can be added: $CV = SD / \text{mean}$ (expressed in %).⁶⁶

Subjective Description

In addition to the objective descriptive parameters, a subjective description of shape (e.g., *spherical*, *conical*, *mushroom-shaped*, *teardrop-shaped*, etc.) and regularity (e.g., *regular*, *with irregular spiky extensions*, etc.) is recommended (Fig. 5).

Pictures

The inclusion of pictures of the coagulation zone is recommended, both in the axial and in the transverse

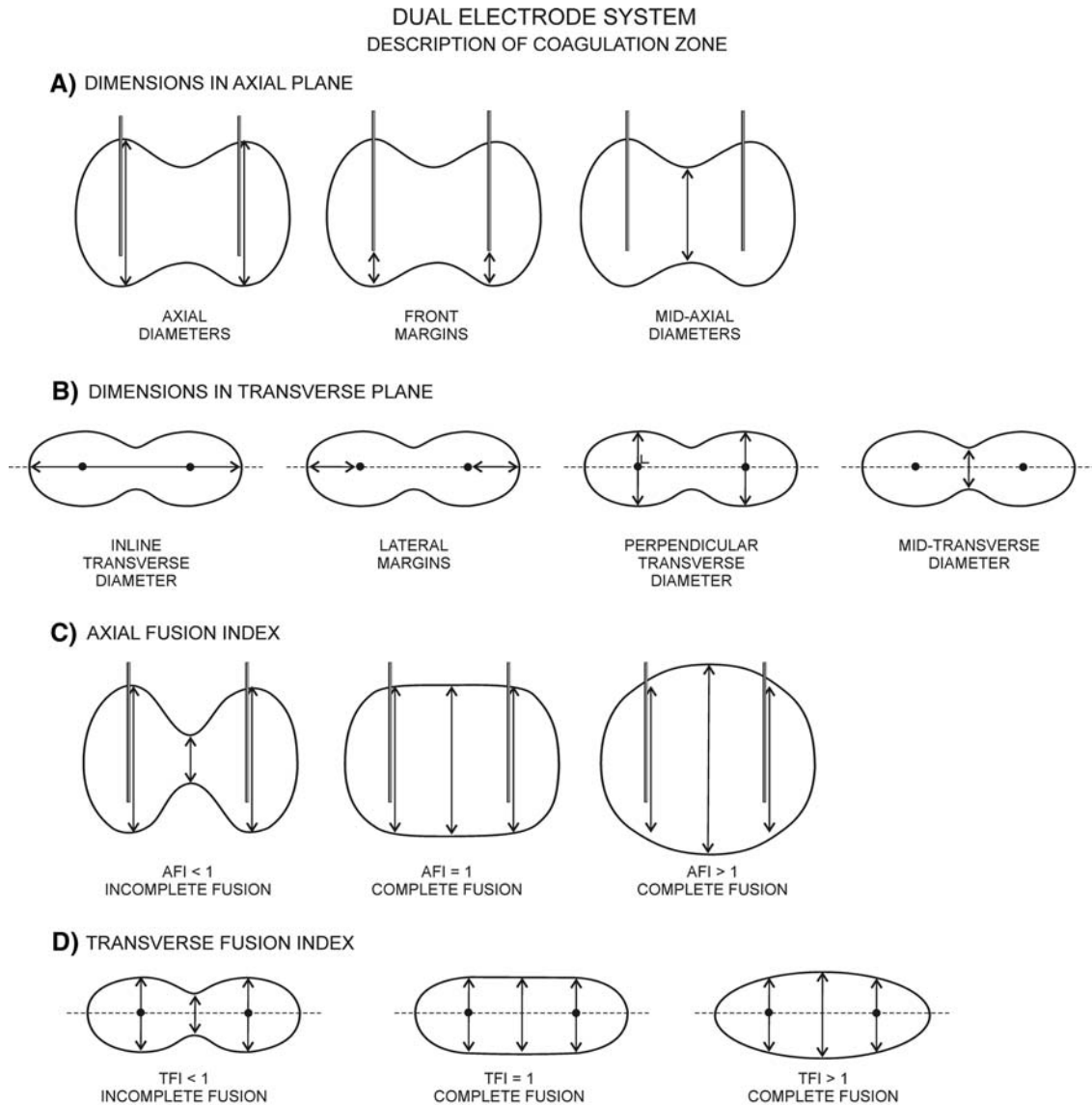


FIG. 4. Description of coagulation zones made by a dual-electrode system.

plane. Pictures shown should be representative of the various sizes and shapes that were obtained with the same electrode and the same protocol. All pictures should be at the same scale and should include a centimeter rule. Three-dimensional imaging reconstructions^{35,67} of the coagulation zone are optional but highly illustrative.

Clinical RF Ablation

Measurement Technique

In order to obtain accurate measurements that can be related to the position of the electrode in the

clinical setting, a prospective registration of the position of the electrode axis and the electrode tip during the procedure is necessary. The inclination of the electrode axis versus the three planes (transverse, sagittal, and coronal) of the patient should be recorded. The position of the electrode tip should be described as accurately as possible in relation to the tumor border and other anatomical landmarks. This information can be completed with imaging registration during the procedure, with the electrode in place.

After the RF ablation, the coagulation zone is defined as the area without contrast uptake on contrast-enhanced computed tomography (CT) or mag-

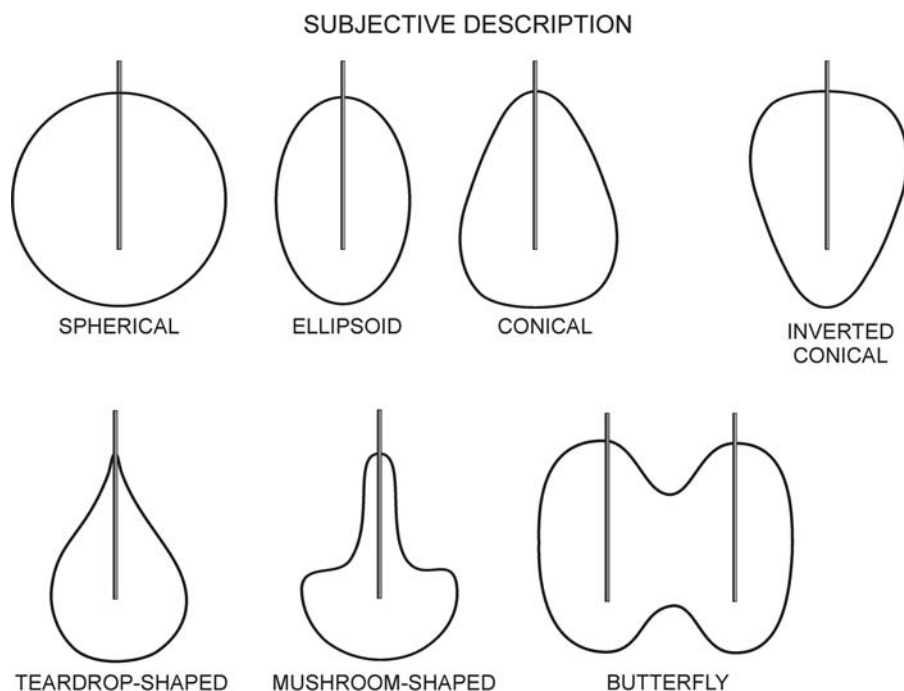


FIG. 5. Subjective description of coagulation zones: some examples.

netic resonance imaging (MRI). The hyperaemic rim is not taken into account.

In a first step, measurements are performed in the *axial plane*, which is defined as a plane along the electrode axis. For CT, this, often oblique, plane has to be reconstructed postimaging using multiplanar reconstruction; a technique which requires a dedicated acquisition protocol with overlapping thin (millimetric) slices, as commonly achievable with recent multidetector helical CTs. The prerecorded inclination values of the electrode axis versus the three patient planes are used for this reconstruction. Measurements of the coagulation zone are performed digitally, and imaging in the axial plane is recorded. With MRI, the plane along the electrode axis can be obtained either through direct oblique acquisition or through secondary multiplanar reformations from transverse thin slices.

Second, measurements are performed in the *transverse plane*, which is defined as the plane perpendicular to the electrode (and to the axial plane) at the site of the largest transverse diameter of the coagulation zone. Measurements of the coagulation zone are performed digitally, and imaging in the axial plane is recorded.

Measurements (Table 3)

Definitions of geometric dimensions are the same for the experimental and the clinical settings. However, as imaging without the electrode in place is

inevitably less accurate than sectioning with the electrode in place, the number of reliable measurements in the clinical setting is smaller. For the same reason, practical application of the geometric definitions in the clinical setting is limited to single RF ablation sessions with a single electrode. In the Material and Methods section of clinical reports, it should be clearly stated that the definitions of “axial” and “transverse” describe the spatial relation with the axis of the electrode and that they should not be confounded with the axial and transverse planes of classical CT or MRI imaging, which describe the spatial relation with the axis of the patient. Further, in clinical reports, the exposant “el” is added to the abbreviations for clarity.

Frequency of Use of Proposed Descriptive Parameters in Experimental RF Ablation Literature

Sixty papers with the main aim describe single-session coagulation zones in animal liver with commercial or experimental electrodes were identified: 50 for a single electrode (Table 4).^{12,21–41,48–55,68–86} Curley (unpublished data) and 10 for a dual-electrode system (Table 5).^{59–65,87,88} For single-electrode experiments, the most essential descriptive parameters, i.e., the axial diameter and the minimal transverse diameter, were available in only 18 and 5 of the 50 papers, respectively. For dual-electrode experiments, the axial diameter, the inline transverse

diameter and the lateral margin were available in only 6, 7, and 0 of the 10 papers, respectively. Forty of 60 papers described *in vivo* experiments. Only 15 of these 40 papers specified whether the red rim was excluded from the measurements: in 13 papers it was excluded, while in 2 papers the red rim was included.

DISCUSSION

In RF ablation of liver tumors, precise tailoring of the size and shape of the coagulation zone is important. The coagulation zone should be large enough to encompass both the tumor and a safety margin of 1 cm at all sides.^{15,16,89} On the other hand, it should be small enough to avoid collateral damage.¹⁷ Real-time ultrasound monitoring of the coagulation zone is unreliable.^{10–13} Diameters measured by ultrasound show a poor correlation with the pathological diameter,^{10–12} with overestimation of the minimal transverse diameter and underestimation of the maximal transverse diameter of the coagulation zone.¹³

MRI and elastography thermometry are promising but still experimental methods for real-time monitoring of tissue temperature and, indirectly, the development of the coagulation zone.^{90–92}

Therefore, knowledge of the expected size and shape of a single-session coagulation zone and its relation to the electrode tip is essential.

A recent review showed that much of this crucial information is lacking for current commercial RF ablation electrodes.¹⁹ This paucity of data was incriminated explicitly as cause of several local recurrences in a recent study.⁹³ The situation is even worse when experimental electrodes are included in the analysis, as shown in the present study (Tables 4 and 5). The development of a minimal set of descriptive parameters and the corresponding expected variation for each RF ablation electrode and protocol may improve the results of RF ablation and will help to avoid the loss of some of its credibility by poor results due to brochure-based overoptimistic expectations of a perfectly spherical coagulation zone with a constant diameter.^{42,94}

This report should be seen as complementary to several recent efforts to standardize reporting on RF ablation. A paper from the International Working Group on Image-Guided Tumor Ablation (IWGIG-TA) proposes standardized terms for general aspects in the broad field of image-guided tumor ablation.⁹⁵ Other papers specifically focused on standardization of one particular aspect of RF ablation, such as a scoring system for complications⁹⁶ and a logical ter-

minology for RF electrodes and RF electrode systems.²⁰ All these efforts are crucial to improve scientific communication in the field of RF ablation.

The proposed terminology has been developed to describe RF coagulation zones but can also be applied to coagulation zones created by other interstitial techniques that use an applicator, such as microwave antennas, laser fibers, and cryoprobes.

Limitations

The current proposal deals only with a standardized macroscopic description of coagulation zones. The exact generator type, electrode type, and treatment algorithm should be documented as well. In order to reliably compare coagulation zones obtained by different electrodes and protocols, a standardized experimental setup is necessary, e.g., regarding the time interval between RF ablation and the measurements; but this falls out of the scope of this report.

The proposed standardized description method may give the impression that size and geometry of coagulation zones are very predictable. In fact, as several authors have recently shown,^{19,67,94,97} variability of coagulation size and geometry remains an important problem, even when using standardized treatment protocols. Description of this variability is an integral part of the current proposal and should be considered as important as the description of the “mean” size and geometry.

The feasibility of the proposed algorithm for reconstructing the original axes of the electrode on follow-up CT scans needs to be assessed.

Predictive Value of Experimental Measurements

The predictive value of data on size and geometry obtained in animal experiments using the proposed description method is high only for the experimental setting in which the data were measured. Size and geometry obtained in *ex vivo* experiments tend to overestimate the coagulation diameter and volume and underestimate variations in geometry compared to *in vivo* experiments.³⁴ Results from *ex vivo* experiments are useful only as a first step to optimize RF technology in the laboratory. Before clinical application of a new electrode or protocol, coagulation size and geometry should always be assessed in *in vivo* experimental studies. Even *in vivo*, the results obtained in the ideal situation, i.e., in the middle of the parenchyma, are not necessarily predictive for the result near a large vessel or near the capsule. Furthermore, findings in animal models should be com-

pared to those observed in patients. The in vivo results of RF ablation in healthy animal liver may not be the same as when applied to a tumor and a surrounding rim of nontumorous liver in a patient. The tumor may be hypo- or hypervascular. It may also have different electrical and thermal characteristics as well as a different sensibility to the generated heat. The liver itself may be altered by fibrosis, cirrhosis, or chemotherapy-induced fatty changes. Hydration may differ between patients. The results of RF ablation obtained in one organ are very different from results in other organs, due to differences in vascularity and composition (water, salts, lipids, and proteins). There are well-known differences for kidney (higher salt content and radial blood flow) versus liver (greater uniformity) versus breast or prostate (higher lipid content, i.e., more insulating capacity).⁹⁸

Preparation Technique for Experimental Measurements

The proposed preparation technique carries the advantage that the exact relation of the edges of the coagulation zone to the electrode shaft and the electrode tip can be recorded. This is difficult to impose if the electrode is retracted from the tissue prior to cutting the tissue into slices. Those slices will only by chance be perfectly perpendicular to the electrode track or parallel to the axial plane.

The border of the central tan-white zone should be taken as the border of the coagulation zone. Within this area, all tissue has been shown to be irreversibly damaged.²² The tannish color is due to differential light absorption and reflection by denatured proteins. The surrounding hyperaemic red rim should be excluded from the measurements. This rim still contains viable cells, as proven by histochemical staining and intracellular adenosine triphosphate measurement techniques in the acute phase,²⁰ though some of them may die later (ATP).

Measurements should be performed before histological tissue fixation with associated tissue shrinkage.

Standardization and Interpretation of Terms

Numerous and often contradictory synonyms have been used in the literature for the terms that have been defined in this proposal (Tables 1 and 2). In order to distill the most unequivocal and universally acceptable terms, we first rejected synonyms that suggested a ranking of size, such as “length” and “width”, “long(est) axis” and “short(est) axis”,

“minimum diameter” and “maximum diameter”, because the longest axis does not necessarily correspond to the axial diameter; neither does the shortest axis always correspond to the transverse diameter.^{19,21} We then rejected synonyms that suggested a position in space, such as “vertical diameter”, “height”, and “depth”, because an RF ablation electrode can be inserted in any direction in the laboratory as well as in a patient. Next, from the remaining terms, the most “expressive” term was selected, as was the case for the “ellipticity index (EI)” which is more “intuitively suggestive” than “aspect ratio”⁵⁶ or “shape value”.³⁵ Finally, some lacking terms had to be newly created.

For the interpretation of these terms, we adopted the principle that all terms describe the *spatial relationship* of the coagulation zone *with the electrode* (and not with the patient nor with the treated organ). Therefore, “axial” should be interpreted as “in the axis of the electrode” and “transverse” as “perpendicular to the axis of the electrode.”

Volume Measurements

In many experimental papers, the description of a three-dimensional coagulation zone is *reduced to a single value* for its volume. This may be useful in the laboratory to optimize energy deposition but is not helpful to plan RF ablation as it leaves the physician ignorant about the size and shape of the coagulation zone. On the other hand, *calculating* expected volumes of coagulation zones based on available data on expected axial and transverse diameter can be useful to prevent liver failure when planning RF ablation in patients with limited liver reserve and/or extensive tumor burden. For a perfect ellipsoid, volume is calculated as $(\pi/6) \bullet AD \bullet TD_{\max} \bullet TD_{\min}$.

Random Diameters

In many papers, two or three dimensions of a coagulation zone are measured and reported, e.g., the “longest diameter” and the “shortest diameter,” without reference to the position of the electrode. Especially in the clinical setting, we acknowledge that measuring random diameters is far easier than measuring dimensions in relation to the electrode as described in the above proposal. However, while random diameters may be useful for volume calculation, they are of little value to accurately describe coagulation zone geometry, and they may even be misleading. Although for many electrodes the longest

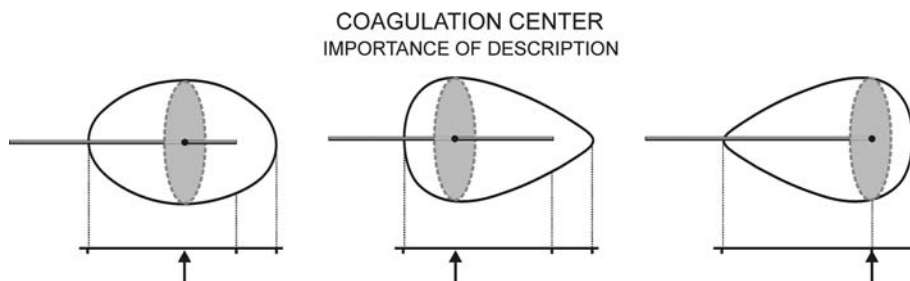


FIG. 6. Importance of description of the position of the coagulation center. These three coagulation zones are quite different despite having the same axial diameter, transverse diameter, and frontal margin. Addition of the position of the coagulation center (arrow) increases accuracy of description.

diameter of the coagulation zone corresponds to the axial diameter, for other electrodes it corresponds to the transverse diameter.^{19,21}

Front Margin

There are no data available to the physician on the front margin, except very recently for the cooled electrode.²² This information, however, is essential to calculate whether the tip of the electrode should be inserted up to the center of a tumor or rather up to the posterior edge or even behind this edge, to ascertain the safety margin.

Awaiting reliable data, the “best guess” of the front margin for straight electrodes may correspond to half the difference between the axial diameter and the length of the noninsulated tip of the electrode, assuming that the coagulation zone is distributed symmetrically at the front and at the back of the active tip.

For expandable electrodes, no “best guess” is possible. For some expandable electrodes, the center of the coagulation zone may correspond to the end of the electrode shaft, while for other expandable electrodes, the center of the coagulation zone is probably deeper into the tissue than the end of the electrode shaft.⁹⁹

Coagulation Center (Fig. 6)

Many coagulation zones are not spherical but rather mushroom- or cone-shaped.³⁵ Moreover, an elongation of the coagulation zone along the electrode track is often observed. In other words, the transverse plane, defined by the maximal transverse diameter in the axial plane, is not always situated halfway between the proximal and distal edges of the coagulation zone in the axial plane. The expected location of the maximal transverse diameter in relation to the tip of the electrode may prove to be a very useful parameter when planning RF ablations in patients.

Maximal and Minimal Transverse Diameter

In some papers, only the maximal transverse diameter of a coagulation zone is measured and reported. The maximal diameter is important to prevent complications by too large coagulation zones¹⁷ but is oncologically irrelevant. In other papers, only the mean of the maximal and minimal transverse diameters or the mean of two perpendicular transverse diameters is reported, which again represents a loss of essential information. Knowledge of the minimal diameter is essential to be sure to cover the tumor and a margin of 1 cm at all sides.

Maximal and Minimal Radius

Knowledge of the radius is more accurate than knowledge of diameter as the radius equals half of the transverse diameter only in symmetrical coagulation zones. Up to 60% of coagulation zones may be asymmetrical.¹² A minimal diameter that has been obtained by measuring asymmetrical coagulation zones represents an overestimation of minimal radius and misleads the clinician. Up to now, no data on maximal and minimal radii of coagulation zones have been available for any electrode. Values for maximal and minimal radii allow calculation of the useful RI (see below).

Ellipticity Index

The EI quantitatively describes the general coagulation zone shape in the axial plane. The higher the index, the more elliptical the coagulation zone, as suggested by the name.¹⁹

Regularity of Shape in the Transverse Plane

The regularity index (RI) quantitatively describes the regularity of the coagulation zone shape in the transverse plane. It is very easy to calculate and clinically relevant. An increasing number of reports

stress the fact that many coagulation zones are less regular than previously assumed.^{19,21,34,35,75,94,97} The numerator of the regularity index is the minimal radius, which is related to the risk of local recurrence,^{15,21,75,97} while the denominator is the maximal radius, which is related to the risk of collateral damage.¹⁷

A ratio close to 1.0 corresponds to a nearly spherical coagulation zone. The lower the ratio, the more irregular the coagulation zone. Because the risk of local recurrence and collateral damage is different for asymmetrical coagulation zones, zones with indentations, or zones with extensions, the (most frequently found) type(s) of irregularity should be specified for RI inferior to 0.80 in the subjective description (see further).

The heat sink effect is common to all electrodes when used with normal blood flow and causes local indentations of the coagulation zone near blood vessels.¹⁹ For coagulation zones created by expandable electrodes, superficial to deep clefts can be present between tines.^{19,75} For coagulation zones made by wet electrodes or its combinations (cooled-wet, expandable-wet, bipolar-wet)²⁰ or by saline-enhanced RF ablation,^{20,100} spiky extensions of the coagulation zone due to irregular spread of saline have been observed.^{34,35,100}

Alternative scoring systems that have been used in the literature to quantify (ir)regularity of coagulation zones include:

- The “Chinn score,” which quantifies clefts between tines on a scale from 0 to 7 but is applicable only to expandable electrodes.^{19,75}
- The “regularity ratio,” which quantifies predictability of coagulation zones on a scale from 0 to 3 but appears to be very subjective.⁶⁴
- The isoperimetric quotient or ratio = $4\pi A/P^2$, where A is the area and P is the perimeter.^{75,101} This score is objective and applicable to all kinds of distortions. Calculating this score, however, is more time consuming as it needs computer analysis of digitalized pictures. Further, it does not allow for discrimination between a clinically acceptable coagulation zone with a saw-tooth edge but minimal variation of the radius and a clinically unacceptable coagulation zone with a smooth edge except for a single deep cleft.

Fusion Index for a Dual-Electrode System

Apart from the objective measurements of the coagulation zone, the single most important

information needed by the clinician is whether coagulation between the two electrodes is complete or not, i.e., whether the coagulation zones around each electrode are completely fused.

Variability

Some reports give only mean values for certain measurements. The standard deviation is essential to assess the range of coagulation zone sizes that one can expect. In a Gaussian distribution, the mean value ± 1 SD includes 68% of observations and the mean value ± 2 SD includes 95% of observations. In other words, the minimal coagulation zone size that can be expected with 97.5% confidence equals the mean size minus 2 standard deviations and the maximal coagulation zone size that can be expected with 97.5% confidence equals the mean size plus 2 standard deviations.

Some papers confuse the reader by describing the *standard error of the mean (SEM)* instead of the *SD*. $SEM = SD/\sqrt{n}$, with n = number of observations. The SEM is a measure for the reliability of the estimation of the mean value of a population by the observed mean value in a sample. It is not at all a measure of variability of the observed values around the observed mean. The SEM is by definition (much) smaller than the SD. Use of the SEM instead of SD gives a false impression of high reproducibility to the statistically less trained reader.

Subjective Description (Fig. 5)

On top of the objective descriptive parameters, a subjective description of shape and regularity is recommended. Examples of shape description include terms such as ellipsoid,³⁵ oval,⁶⁸ ovoid,¹² conical,^{56,68} inverted conical,³⁵ pear-shaped,²⁵ mushroom-shaped,⁷³ droplet-shaped,⁷³ teardrop-shaped,⁹⁴ dumbbell-shaped,^{25,56} and butterfly-shaped⁸⁷.

For single-electrode coagulation zones with an RI < 0.8, the (most frequently found) type(s) of irregularity should be specified: asymmetrical with indentations (including cloverleaf-shaped²⁷ or with deep clefts⁷⁸) or with irregular (flamelike or spiky) extensions.¹⁰⁰ Subjective descriptions of shape and regularity may at first glance seem to be imprecise and unscientific. They are, however, a powerful warning to the clinician against a too optimistic expectation of a regular and spherical coagulation zone for the electrodes and protocols that have been tested.

Pictures

“A picture tells more than a thousand words” is true in this context too. It completes the numerical and subjective description. A picture can disclose an irregular shape that was not obvious with objective measurements. Three-dimensional imaging reconstructions^{35,67} of the coagulation zone are even more illustrative.

CONCLUSIONS

Hopefully, the widespread adoption of this proposed minimal set of descriptive parameters will soon fill in the many gaps in our knowledge about the size and geometry of coagulation zones.

Companies are strongly encouraged to provide this set of data for all RF ablation electrodes that they have or intend to bring on the market. In the liver, these data should be produced with and without the Pringle maneuver, both within a predefined short distance to large intrahepatic vessels as well as in hepatic parenchyma without nearby vessels.

A better recognition of shortcomings in size, shape, and regularity of coagulation zones produced by the actual RF ablation electrodes may lead to less local recurrence and collateral damage and may boost research to improve these features.

ACKNOWLEDGMENT

The authors thank Marie-Bernadette Jacqmain and Christian Deneffe for the illustrations.

REFERENCES

- Curley SA, Izzo F, Delrio P, et al. Radiofrequency ablation of unresectable primary and metastatic hepatic malignancies. Results in 123 patients. *Ann Surg* 1999; 230:1–8.
- Siperstein A, Garland A, Engle K, et al. Local recurrence after laparoscopic radiofrequency thermal ablation of hepatic tumors. *Ann Surg Oncol* 2000; 7:106–113.
- Bleicher RJ, Allegra DP, Nora DT, Wood TF, Foshag LJ, Bilchik AJ. Radiofrequency ablation in 447 complex unresectable liver tumors: lessons learned. *Ann Surg Oncol* 2003; 10:52–58.
- Pawlik TM, Izzo F, Cohen DS, Morris JS, Curley SA. Combined resection and radiofrequency ablation for advanced hepatic malignancies: results in 172 patients. *Ann Surg Oncol* 2003; 10:1059–1069.
- Elias D, Baton O, Sideris L, Matsuhisa T, Pocard M, Lasser P. Local recurrences after intraoperative radiofrequency ablation of liver metastases: a comparative study with anatomic and wedge resections. *Ann Surg Oncol* 2004; 11:500–505.
- Poon RT, Ng KK, Lam CM, Ai V, Yuen J, Fan ST. Radiofrequency ablation for subcapsular hepatocellular carcinoma. *Ann Surg Oncol* 2004; 11:281–289.
- Raut CP, Izzo F, Marra P, et al. Significant long-term survival after radiofrequency ablation of unresectable hepatocellular carcinoma in patients with cirrhosis. *Ann Surg Oncol* 2005; 12:616–628.
- Gervais DA, McGovern FJ, Arellano RS, McDougal WS, Mueller PR. Radiofrequency ablation of renal cell carcinoma. Part 1: Indications, results, and role in patient management over a 6-year period and ablation of 100 tumors. *Am J Roentgenol* 2005; 185:64–71.
- Shariat SF, Raptidis G, Masatoschi M, Bergamaschi F, Slatin KM. Pilot study of radiofrequency interstitial tumor ablation (RITA) for the treatment of radio-recurrent prostate cancer. *Prostate* 2005; 65:260–267.
- Cha CH, Lee FT, Gurney JM, et al. CT versus sonography for monitoring radiofrequency ablation in a porcine liver. *AJR Am J Roentgenol* 2000; 175:705–711.
- Raman SS, Lu DSK, Vodopich DJ, Sayre J, Lassman C. Creation of radiofrequency lesions in a porcine model: correlation with sonography, CT and histopathology. *Am J Roentgenol* 2000; 175:1253–1258.
- Scott DJ, Fleming JB, Watumull LM, Lindberg G, Tesfay ST, Jones DB. The effect of hepatic inflow occlusion on laparoscopic radiofrequency ablation using simulated tumors. *Surg Endosc* 2002; 16:1286–1291.
- Leyendecker JR, Dodd GD 3rd, Halff GA, et al. Sonographically observed echogenic response during intraoperative radiofrequency ablation of cirrhotic livers: pathologic correlation. *Am J Roentgenol* 2002; 178:1147–1151.
- Kuvshinov BW, Ota DM. Radiofrequency ablation of liver tumors: influence of technique and tumor size. *Surgery* 2002; 132:605–611.
- Mulier S, Ni T, Jamart J, Ruers T, Marchal G, Michel L. Local recurrence after hepatic radiofrequency coagulation—multivariate meta-analysis and review of contributing factors. *Ann Surg* 2005; 242:158–171.
- Wood TF, Rose DM, Chung M, Allegra DP, Foshag LJ, Bilchik AJ. Radiofrequency ablation of 231 unresectable hepatic tumors: indications, limitations, and complications. *Ann Surg Oncol* 2000; 7:593–600.
- Mulier S, Mulier P, Ni Y, et al. Complications of radiofrequency coagulation of liver tumours. *Br J Surg* 2002; 89:1206–1222.
- Johnson DB, Solomon SB, Su LM, et al. Defining the complications of cryoablation and radiofrequency ablation of small renal tumors: a multi-institutional review. *J Urol* 2004; 172:874–877.
- Mulier S, Ni Y, Miao Y, et al. Size and geometry of hepatic radiofrequency lesions. *Eur J Surg Oncol* 2003; 29:867–878.
- Mulier S, Miao Y, Mulier P, et al. Electrodes and multiple electrode systems for radiofrequency ablation: a proposal for updated terminology. *Eur Radiol* 2005; 15:798–808.
- de Baere T, Denys A, Johns Wood B, et al. Radiofrequency liver ablation: experimental comparative study of water-cooled versus expandable systems. *Am J Roentgenol* 2001; 176:187–192.
- Ng KK, Lam CM, Poon RT, et al. Porcine liver: morphologic characteristics and cell viability at experimental radiofrequency ablation with internally cooled electrodes. *Radiology* 2005; 235:478–486.
- Rossi S, Fornari F, Pathies C, Buscarini L. Thermal lesions induced by 480 kHz localized current field in guinea pig and pig liver. *Tumori* 1990; 76:54–57.
- Goldberg SN, Gazelle GS, Dawson SL, Rittman WJ, Mueller PR, Rosenthal DI. Tissue ablation with radiofrequency: effect of probe size, gauge, duration, and temperature on lesion volume. *Acad Radiol* 1995; 2:399–404.
- Goldberg SN, Gazelle GS, Halpern EF, Rittman WJ, Mueller PR, Rosenthal DI. Radiofrequency tissue ablation: importance of local temperature along the electrode tip exposure in

- determining lesion shape and size. *Acad Radiol* 1996; 3:212–218.
26. Lorentzen T, Christensen NEH, Nolsøe CP, Torp Pedersen ST. Radiofrequency tissue ablation with a cooled needle in vitro: ultrasonography, dose response, and lesion temperature. *Acad Radiol* 1997; 4:292–297.
 27. Patterson EJ, Scudamore CH, Owen DA, Nagy AG, Buczkowski AK. Radiofrequency ablation of porcine liver in vivo. Effects of blood flow and treatment time on lesion size. *Ann Surg* 1998; 227:559–565.
 28. Hänslér J, Becker D, Müller W, Neureiter D, Hahn EG. Ultraschallgesteuerte Hochfrequenz Thermotheapie (HFTT). In vitro Untersuchung an der Rinderleber. *Ultraschall Med* 1998; 19:59–63.
 29. Goldberg SN, Hahn PF, Tanabe KK, et al. Percutaneous radiofrequency tissue ablation: does perfusion mediated tissue cooling limit coagulation necrosis?. *J Vasc Interv Radiol* 1998; 9:101–111.
 30. Scott DJ, Young WN, Watumull LM, et al. Accuracy and effectiveness of laparoscopic vs open hepatic radiofrequency ablation. *Surg Endosc* 2001; 15:135–140.
 31. Chang CK, Hendy MP, Smith JM, Recht MH, Welling RE. Radiofrequency ablation of the porcine liver with complete hepatic vascular occlusion. *Ann Surg Oncol* 2002; 9:594–598.
 32. Hänslér J, Neureiter D, Strobel D, et al. Cellular and vascular reactions in the liver to radio-frequency thermo-ablation with wet needle applicators: study on juvenile domestic pigs. *Eur Surg Res* 2002; 34:357–363.
 33. Schmidt D, Trubenbach J, Brieger J, et al. Automated saline-enhanced radiofrequency thermal ablation: initial results in ex vivo bovine livers. *Am J Roentgenol* 2003; 180:163–165.
 34. Denys AL, De Baere T, Kuoch V, et al. Radio-frequency tissue ablation of the liver: in vivo and ex vivo experiments with four different systems. *Eur Radiol* 2003; 13:2346–2352.
 35. Pereira PL, Trubenbach J, Schenk M, et al. Radiofrequency ablation: in vivo comparison of four commercially available devices in pig livers. *Radiology* 2004; 232:482–490.
 36. Watanabe S, Kurokohchi K, Masaki T, et al. Enlargement of thermal ablation zone by the combination of ethanol injection and radiofrequency ablation in excised bovine liver. *Int J Oncol* 2004; 24:279–284.
 37. Lee JM, Lee YH, Kim YK, Kim SW, Kim CS. Combined therapy of radiofrequency ablation and ethanol injection of rabbit liver: an in vivo feasibility study. *Cardiovasc Intervent Radiol* 2004; 27:151–157.
 38. Lee JM, Kim YK, Kim SW, Han JK, Kim SH, Choi BI. Combined radiofrequency ablation and acetic acid hypertonic saline solution instillation: an in vivo study of rabbit liver. *Korean J Radiol* 2004; 5:31–38.
 39. Kim SK, Lim HK, Ryu JA, et al. Radiofrequency ablation of rabbit liver in vivo: effect of the pringle maneuver on pathologic changes in liver surrounding the ablation zone. *Korean J Radiol* 2004; 5:240–249.
 40. Lee JM, Han JK, Kim SH, et al. Optimization of wet radiofrequency ablation using a perfused-cooled electrode: a comparative study in ex vivo bovine livers. *Korean J Radiol* 2004; 5:250–257.
 41. Lee JM, Han JK, Kim SH, et al. Comparison of wet radiofrequency ablation with dry radiofrequency ablation and radiofrequency ablation using hypertonic saline preinjection: ex vivo bovine liver. *Korean J Radiol* 2004; 5:258–265.
 42. Lobik L, Leveillee RJ, Hoey MF. Geometry and temperature distribution during radiofrequency tissue ablation: an experimental ex vivo model. *J Endourol* 2005; 19:242–247.
 43. Steiner P, Botnar R, Goldberg SN, Gazelle GS, Debatin JF. Monitoring of radiofrequency tissue ablation in an interventional magnetic resonance environment. Preliminary ex vivo and in vivo results. *Invest Radiol* 1997; 32:671–678.
 44. Steiner P, Botnar R, Dubno B, Zimmermann GG, Gazelle GS, Debatin JF. Radiofrequency induced thermoablation: monitoring with T1 weighted and proton frequency shift MR imaging in an interventional 0.5 T environment. *Radiology* 1998; 206:803–810.
 45. Tungjitkusolmun S, Staelin ST, Haemmerich D, et al. Three-dimensional finite-element analyses for radio-frequency hepatic tumor ablation. *IEEE Trans Biomed Eng* 2002; 49:3–9.
 46. Varghese T, Techavipoo U, Liu W, et al. Elastographic measurement of the area and volume of thermal lesions resulting from radiofrequency ablation: pathologic correlation. *AJR Am J Roentgenol* 2003; 181:701–707.
 47. Lorentzen T. A cooled needle electrode for radiofrequency tissue ablation: thermodynamic aspects of improved performance compared with conventional needle design. *Acad Radiol* 1996; 3:556–563.
 48. Goldberg SN, Stein MC, Gazelle GS, Sheiman RG, Kruskal JB, Clouse ME. Percutaneous radiofrequency tissue ablation: optimization of pulsed radiofrequency technique to increase coagulation necrosis. *J Vasc Interv Radiol* 1999; 10:907–916.
 49. Denys AL, de Baere T, Mahe C, et al. Radiofrequency tissue ablation of the liver: effects of vascular occlusion on lesion diameter and biliary and portal damages in a pig model. *Eur Radiol* 2001; 11:2102–2108.
 50. Goldberg SN, Ahmed M, Gazelle GS, et al. Radio-frequency thermal ablation with NaCl solution injection: effect of electrical conductivity on tissue heating and coagulation phantom and porcine liver study. *Radiology* 2001; 219:157–165.
 51. Haemmerich D, Chachati L, Wright AS, Mahvi DM, Lee FT Jr, Webster JG. Hepatic radiofrequency ablation with internally cooled probes: effect of coolant temperature on lesion size. *IEEE Trans Biomed Eng* 2003; 50:493–500.
 52. Horkan C, Ahmed M, Liu Z, et al. Radiofrequency ablation: effect of pharmacologic modulation of hepatic and renal blood flow on coagulation diameter in a VX2 tumor model. *J Vasc Interv Radiol* 2004; 15:269–274.
 53. Miao Y, Ni Y, Mulier S, et al. Ex vivo experiment on radiofrequency liver ablation with saline infusion through a screw tip cannulated electrode. *J Surg Res* 1997; 71:19–24.
 54. Ni Y, Miao Y, Mulier S, Yu J, Baert AL, Marchal G. A novel “cooled-wet” electrode for radiofrequency ablation. *Eur Radiol* 2000; 10:852–854.
 55. Miao Y, Ni Y, Yu J, Marchal G. A comparative study on validation of a novel cooled-wet electrode for radiofrequency ablation. *Invest Radiol* 2000; 35:438–444.
 56. Chung YC, Duerk JL, Lewin JS. Generation and observation of radiofrequency thermal lesion ablation for interventional magnetic resonance imaging. *Invest Radiol* 1997; 32:466–474.
 57. Pereira PL, Clasen S, Boss A, et al. Radiofrequency ablation of liver metastases. *Radiologie* 2004; 44:347–357.
 58. Lee JM, Han JK, Kim SH, et al. A comparative experimental study of the in-vitro efficiency of hypertonic saline-enhanced hepatic bipolar and monopolar radiofrequency ablation. *Korean J Radiol* 2003; 4:163–169.
 59. Lee JM, Han JK, Kim SH, et al. Saline-enhanced hepatic radiofrequency ablation using a perfused-cooled electrode: comparison of dual probe bipolar mode with monopolar and single probe bipolar modes. *Korean J Radiol* 2004; 5:121–127.
 60. Lee JM, Rhim H, Han JK, Youn BJ, Kim SH, Choi BI. Dual-probe radiofrequency ablation: an in vitro experimental study in bovine liver. *Invest Radiol* 2004; 39:89–96.
 61. Lee JM, Han JK, Kim SH, Sohn KL, Choi SH, Choi BI. Bipolar radiofrequency ablation in ex vivo bovine liver with the open-perfused system versus the cooled-wet system. *Eur Radiol* 2005; 15:759–764.
 62. Lee JM, Han JK, Kim SH, et al. Bipolar radiofrequency ablation using wet-cooled electrodes: an in vitro experimental study in bovine liver. *AJR Am J Roentgenol* 2005; 184:391–397.

63. Burdio F, Guemes A, Burdio JM, et al. Bipolar saline-enhanced electrode for radiofrequency ablation: results of experimental study of in vivo porcine liver. *Radiology* 2003; 229:447–456.
64. Burdio F, Guemes A, Burdio JM, et al. Large hepatic ablation with bipolar saline-enhanced radiofrequency: an experimental study in in vivo porcine liver with a novel approach. *J Surg Res* 2003; 110:193–201.
65. Lee JM, Han JK, Kim SH, Lee JY, Choi SH, Choi BI. Hepatic bipolar radiofrequency ablation using perfused-cooled electrodes: a comparative study in the ex vivo bovine liver. *Br J Radiol* 2004; 77:944–949.
66. Bahn AK. (1972) Basic Medical Statistics Grune and Stratton, New York, p 105
67. Frich L, Mala T, Gladhaug IP. Hepatic radiofrequency ablation using perfusion electrodes in a pig model: effect of the Pringle manoeuvre. *Eur J Surg Oncol* 2006.
68. Sanchez R, Van Sonnenberg E, D'Agostino H, Goodacre B, Esch O. Percutaneous tissue ablation by radiofrequency thermal energy as a prelude to tumour ablation. *Minim Invasive Ther* 1993; 2:299–305.
69. Nativ O, Moskovitz B, Sabo E, et al. Percutaneous ablation of malignant liver tumor in rabbits using low radiofrequency energy. *J Exp Ther Oncol* 1996; 1:312–316.
70. Trübenbach J, Huppert PE, Pereira PL, Ruck P, Claussen CD. Radiofrequency ablation of the liver in vitro: increasing the efficacy by perfusion probes. *Rofo Fortschr Geb Rontgenstr Neuen Bildgeb Verfahr* 1997; 167:633–637.
71. Hansen PD, Rogers S, Corless CL, Swanstrom LL, Siperstein AE. Radiofrequency ablation lesions in a pig liver model. *J Surg Res* 1999; 87:114–121.
72. Rossi S, Garbagnati F, De Francesco I, et al. Relationship between the shape and size of radiofrequency induced thermal lesions and hepatic vascularization. *Tumori* 1999; 85:137–141.
73. Shibata T, Niinobu T, Ogata N. Comparison of the effects of in vivo thermal ablation of pig liver by microwave and radiofrequency coagulation. *J Hepatobiliary Pancreat Surg* 2000; 7:592–598.
74. Horigome H, Nomura T, Saso K, et al. Percutaneous radiofrequency ablation therapy using a clustered electrode in the animal liver. *Hepatogastroenterology* 2001; 48:163–165.
75. Chinn SB, Lee FT Jr, Kennedy GD, et al. Effect of vascular occlusion on radiofrequency ablation of the liver: results in a porcine model. *AJR Am J Roentgenol* 2001; 176:789–795.
76. Aschoff AJ, Merkle EM, Wong V, et al. How does alteration of hepatic blood flow affect liver perfusion and radiofrequency induced thermal lesion size in rabbit liver?. *J Magn Reson Imaging* 2001; 13:57–63.
77. Miao Y, Ni Y, Yu J, Zhang H, Baert A, Marchal G. An ex vivo study on radiofrequency tissue ablation: increased lesion size by using an “expandable-wet” electrode. *Eur Radiol* 2001; 11:1841–1847.
78. Sugimori K, Morimoto M, Shirato K, et al. Radiofrequency ablation in a pig liver model: effect of transcatheter arterial embolization on coagulation diameter and histologic characteristics. *Hepatol Res* 2002; 24:164–173.
79. Lee JM, Kim YK, Lee YH, Kim SW, Li CA, Kim CS. Percutaneous radiofrequency thermal ablation with hypertonic saline injection: in vivo study in a rabbit liver model. *Korean J Radiol* 2003; 4:27–34.
80. Kim YK, Lee JM, Kim SW, Kim CS. Combined radiofrequency ablation and hot saline injection in rabbit liver. *Invest Radiol* 2003; 38:725–732.
81. Wiersinga WJ, Jansen MC, Straatsburg IH, et al. Lesion progression with time and the effect of vascular occlusion following radiofrequency ablation of the liver. *Br J Surg* 2003; 90:306–312.
82. Shen P, Fleming S, Westcott C, Challa V. Laparoscopic radiofrequency ablation of the liver in proximity to major vasculature: effect of the Pringle maneuver. *J Surg Oncol* 2003; 83:36–41.
83. Lee JM, Lee YH, Kim YK, et al. Combined treatment of radiofrequency ablation and acetic acid injection: an in vivo feasibility study in rabbit liver. *Eur Radiol* 2004; 14:1303–10.
84. Schmidt D, Trubenbach J, Konig CW, et al. Radiofrequenzablation ex-vivo: Vergleich der Effektivität von impedance control mode versus manual control mode unter Verwendung einer geschlossen perfundierten Cluster-Ablationssonde. *Rofo Fortschr Geb Rontgenstr Neuen Bildgeb Verfahr* 2003; 175:967–972.
85. Tamaki K, Shimizu I, Oshio A, et al. Influence of large intrahepatic blood vessels on the gross and histological characteristics of lesions produced by radiofrequency ablation in a pig liver model. *Liver Int* 2004; 24:696–701.
86. Smith MK, Mutter D, Forbes LE, Mulier S, Marescaux J. The physiologic effect of the pneumoperitoneum on radiofrequency ablation. *Surg Endosc* 2004; 18:35–38.
87. McGahan JP, Gu WZ, Brock JM, Tesluk H, Jones CD. Hepatic ablation using bipolar radiofrequency electrocautery. Preliminary investigation. *Acad Radiol* 1996; 3:418–422.
88. Burdio F, Guemes A, Burdio JM, et al. Hepatic lesion ablation with bipolar saline-enhanced radiofrequency in the audible spectrum. *Acad Radiol* 1999; 6:680–686.
89. Curley SA, Izzo F. Laparoscopic radiofrequency. *Ann Surg Oncol* 2000; 7:78–79.
90. Frich L. Non-invasive thermometry for monitoring hepatic radiofrequency ablation. *Minim Invasive Ther All Technol* 2006; 15:18–25.
91. Vigen KK, Jarrard J, Rieke V, Frisoli J, Daniel BL, Pauly KB. In vivo porcine liver radiofrequency ablation with simultaneous MR temperature imaging. *J Magn Reson Imaging* 2006; 23:578–584.
92. Varghese T, Daniels MJ. Real-time calibration of temperature estimates during radiofrequency ablation. *Ultrason Imaging* 2004; 26:185–200.
93. Poon RT, Ng KK, Lam CM, Ai V, Yuen J, Fan ST, Wong J. Learning curve for radiofrequency ablation of liver tumors: prospective analysis of initial 100 patients in a tertiary institution. *Ann Surg* 2004; 239:441–449.
94. Stippel DL, Brochhagen HG, Arenja M, Hunkemoller J, Holscher AH, Beckurts KT. Variability of size and shape of necrosis induced by radiofrequency ablation in human livers: a volumetric evaluation. *Ann Surg Oncol* 2004; 11:420–425.
95. Goldberg SN, Grassi CJ, Cardella JF, et al. Image-guided tumor ablation: standardization of terminology and reporting criteria. *Radiology* 2005; 235:728–739.
96. Omary RA, Bettmann MA, Cardella JF, et al. Quality improvement guidelines for the reporting and archiving of interventional radiology procedures. *J Vasc Interv Radiol* 2003; 14:S293–295.
97. Montgomery RS, Rahal A, Dodd GD 3rd, Leyendecker JR, Hubbard LG. Radiofrequency ablation of hepatic tumors: variability of lesion size using a single ablation device. *AJR Am J Roentgenol* 2004; 182:657–661.
98. Leveillee RJ, Hoey MF. Radiofrequency interstitial tissue ablation: wet electrode. *J Endourol* 2003; 17:563–577.
99. Berber E, Flesher NL, Siperstein AE. Initial clinical evaluation of the RITA 5-centimeter radiofrequency thermal ablation catheter in the treatment of liver tumors. *Cancer J* 2000; 6(suppl 4):S319–295.
100. Ni Y, Mulier S, Miao Y, Michel L, Marchal G. A review of the general aspects of radiofrequency ablation. *Abdom Imaging* 2005; 30:381–400.
101. Haemmerich D, Lee FT Jr, Schutt DJ, et al. Large-volume radiofrequency ablation of ex vivo bovine liver with multiple cooled cluster electrodes. *Radiology* 2005; 234:563–568.

Current address of Stefaan Mulier :

Stefaan Mulier, MD

Philipslaan 66

3000 Leuven

Belgium

+32 16 35 67 86

+32 498 78 73 57

stefaan.mulier@skynet.be

<http://drmulier.com/research.html>